Supplementary Figures

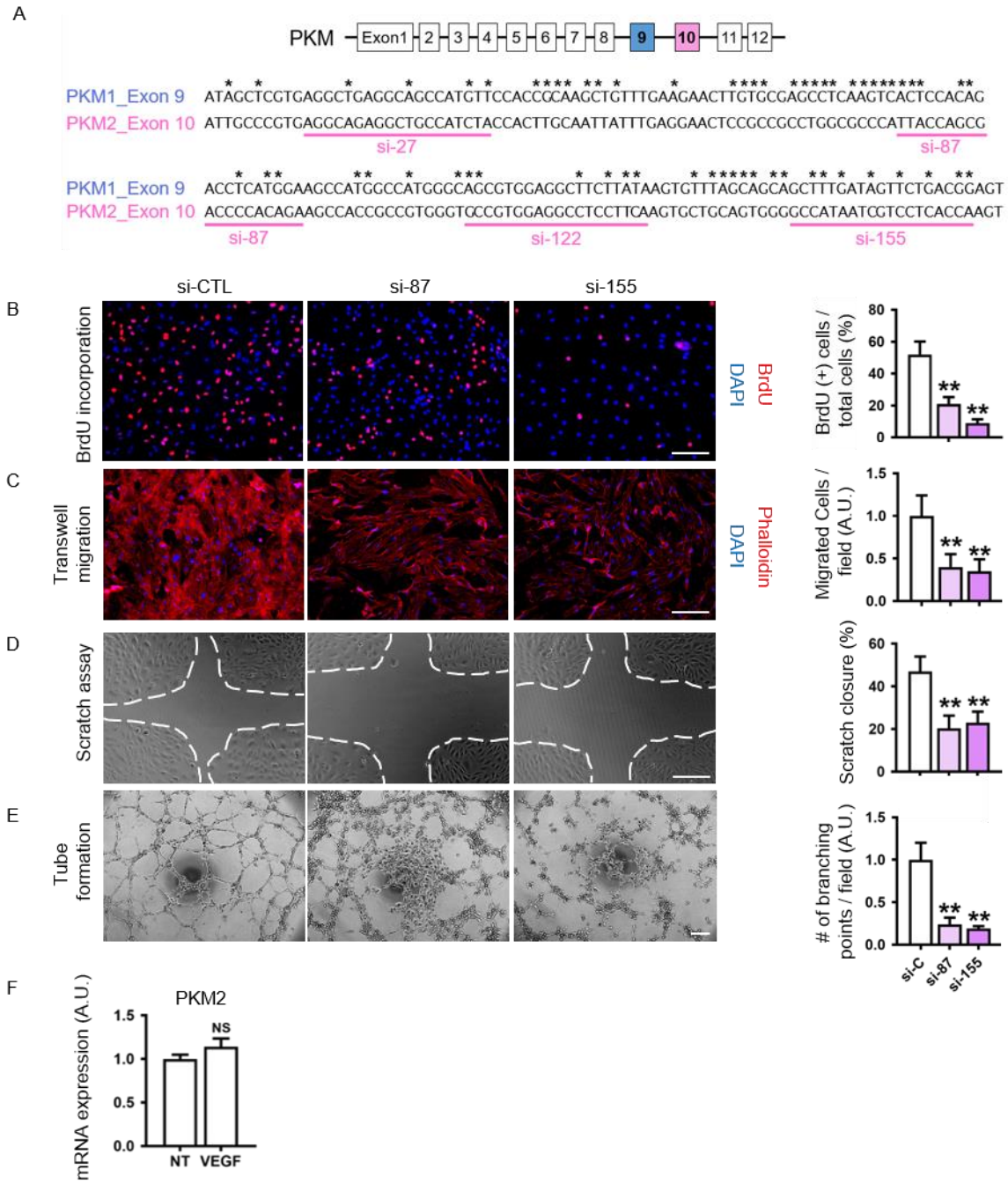

Supplementary Figure 1. Schematic of PKM2-specific siRNAs and their effect on proliferation and migration.

(A) The sequences of Exon 9 and 10 that encodes PKM1 and PKM2, respectively, are shown with asterisks above mismatches. The target sequences of the four different si-RNAs are underlined in pink. (B) Percentage of BrdU-positive cells are reduced by si-87 and si-155. This

experiment was done at the same time as shown in Figure 1D, and therefore the si-CTL data are the same. For si-CTL, the same data set shown in Figure 1D was re-presented. $n = 3$. (C) Reduction in transwell migration of ECs by si-87 and si-155. Cells that migrated across the transwell membrane were visualized by staining with phalloidin (red) and DAPI (blue). This experiment was done at the same time as shown in Figure 1F, and therefore the si-CTL data are the same. $n = 3$. (D) Scratch closure was retarded in ECs with si-87 and si-155. $n = 3$. This experiment was done at the same time as shown in Figure 1G, and therefore the si-CTL data are the same. $n = 3$. (E) Tube formation on matrigel was impaired in ECs with si-87 and si-155. $n = 3$. (F) VEGF (10ng/ml for 12 hour) treatment does not affect PKM2 expression. Scale bar = 100 μm. All data are represented as mean ± STDEV. $^{**}P < 0.01$, by two-tailed Student's *t*-test.

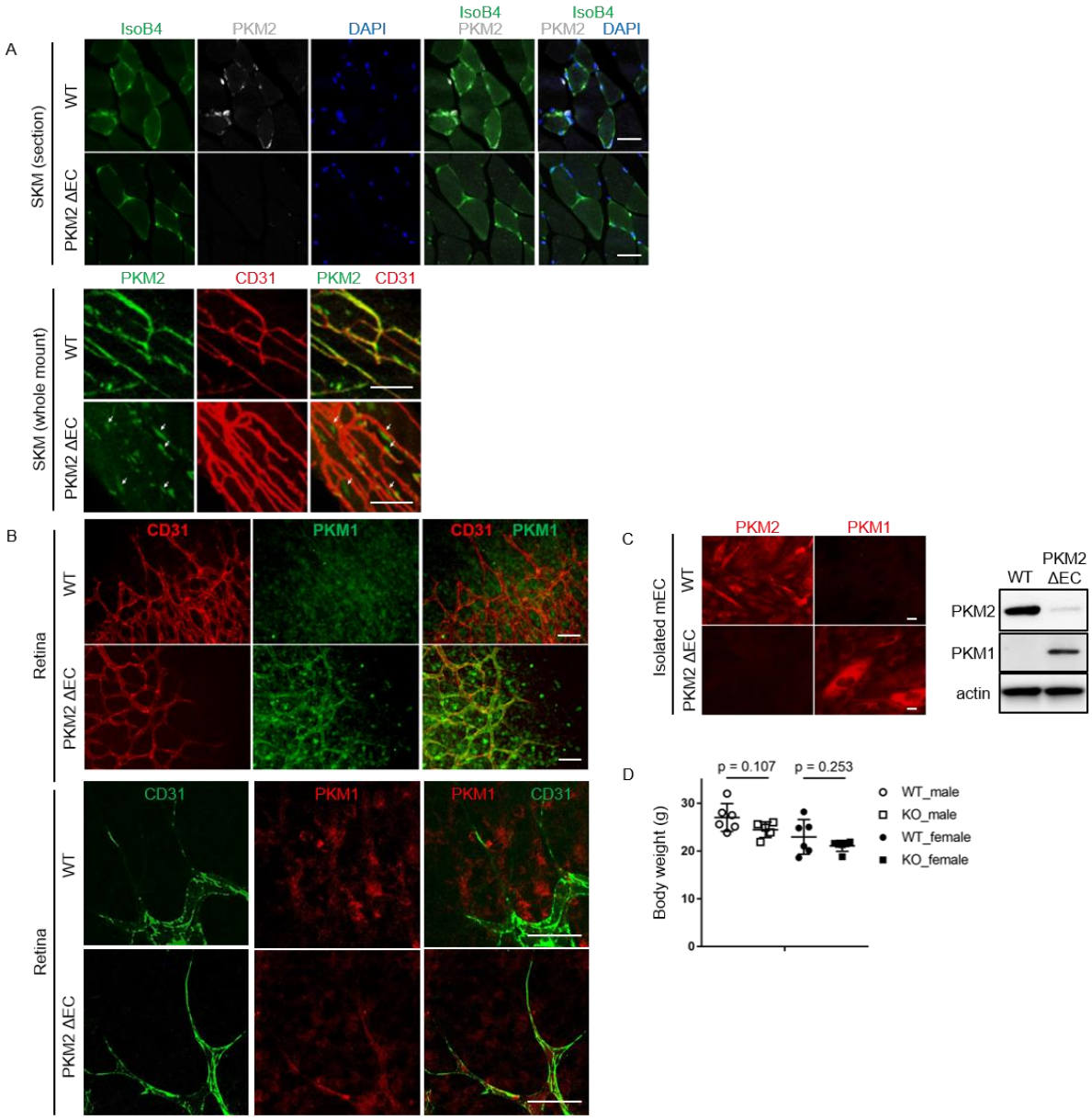

Supplementary Figure2. Validation of EC-specific PKM2 knockout mice.

(A) Cross sectional staining of skeletal muscle (SKM, soleus) with IsoB4 (green), PKM2 (white), and DAPI (blue) in WT vs PKM2$^{\Delta EC}$ mice (upper panel). Whole-mount staining of SKM with PKM2 (green) and CD31 (red) (lower panel). White arrows indicate non-EC cells expressing PKM2 in PKM2$^{\Delta EC}$ mice. Scare bar = 50 µm. (B) Retinal staining (upper panel: 20x and lower panel: 40x) of P7 WT vs PKM2 PKM2$^{\Delta EC}$ mouse with CD31 (red) and PKM1 (green) demonstrating induction of PKM1 expression in ECs of PKM2$^{\Delta EC}$ mice. Scale bar = 50 µm. (C) Immunocytochemistry (left panel) and Western blot analysis (right panel) of isolated ECs from WT vs PKM2$^{\Delta EC}$ mouse with PKM2 or PKM1 antibody confirms nearly complete knock out of PKM2 protein and induction of PKM1 protein in the PKM2$^{\Delta EC}$ mice. Scale bar = 10 µm. (D) Body

weight of 15 week old PKM2$^{\Delta EC}$ mouse as compared to WT littermate controls. Data are presented as mean ± STDEV, n = 6.

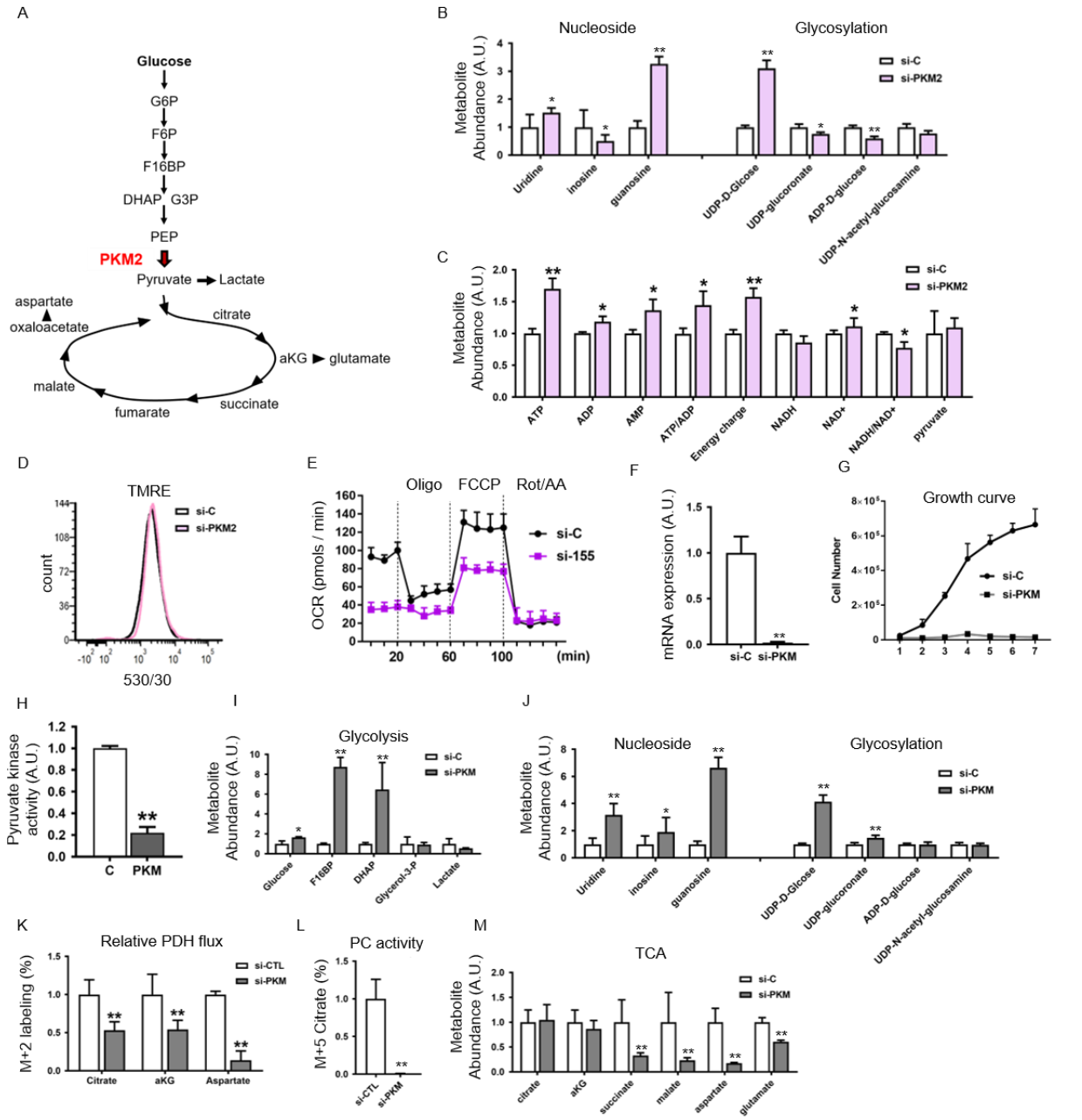

Supplementary Figure 3. Knockdown of PKM phenocopies PKM2 knockdown.

(A) Schematic illustration demonstrating upstream and downstream metabolic pathways of pyruvate kinase. (B) Relative abundance of metabolites that are upstream of PKM in glycolysis in HUVECs with si-C vs si-PKM2 were quantified by mass spectrometry after 24 hrs of incubation. *n* = 3. (C) Relative abundance of ATP, ADP, AMP, ATP/ADP ratio, energy charge (ATP+1/2ADP / ATP+ADP+AMP), NADH, NAD+, NADH/NAD+, and pyruvate was quantified by mass spectrometry. *n* = 3. (D) Mitochondrial membrane potential of HUVECs with si-C vs si-PKM2 was measured by flow cytometry after TMRE staining. The data represents 3 independent experiments. (E) Oxygen consumption rate (OCR) of HUVECs with si-C vs si-155

was measured by Seahorse. n = 8. (F) qPCR analysis of PKM mRNA level in HUVECS with si-C vs si-PKM. n = 3. (G) Growth curve demonstrating complete inhibition of proliferation in si-PKM HUVECs. n = 4. (H) Pyruvate kinase activity assay in HUVECS with si-C vs si-PKM. n = 3. (I) Relative abundance of glycolysis intermediates in HUVECs with si-C vs si-PKM were quantified by mass spectrometry after 24 hrs of incubation. n = 3. (J) Relative abundance of metabolites that are upstream of PKM in glycolysis in HUVECs with si-C vs si-PKM were quantified by mass spectrometry after 24 hrs of incubation. n = 3. (K) Relative PDH activity estimated by incorporation of [U-^{13}C] glucose into M+2 citrate, αKG, and aspartate in HUVECs with si-C vs si-PKM. n = 3. (L) Pyruvate carboxylase (PC) activity estimated by incorporation of [U-^{13}C] glucose into M+5 citrate. n = 3. (M) Relative abundance of TCA cycle intermediates in HUVECs with si-C vs si-PKM were quantified by mass spectrometry after 24 hrs of incubation. n = 3. All data are represented as mean ± STDEV. *P < 0.05. **P < 0.01, by two-tailed Student's t-test.

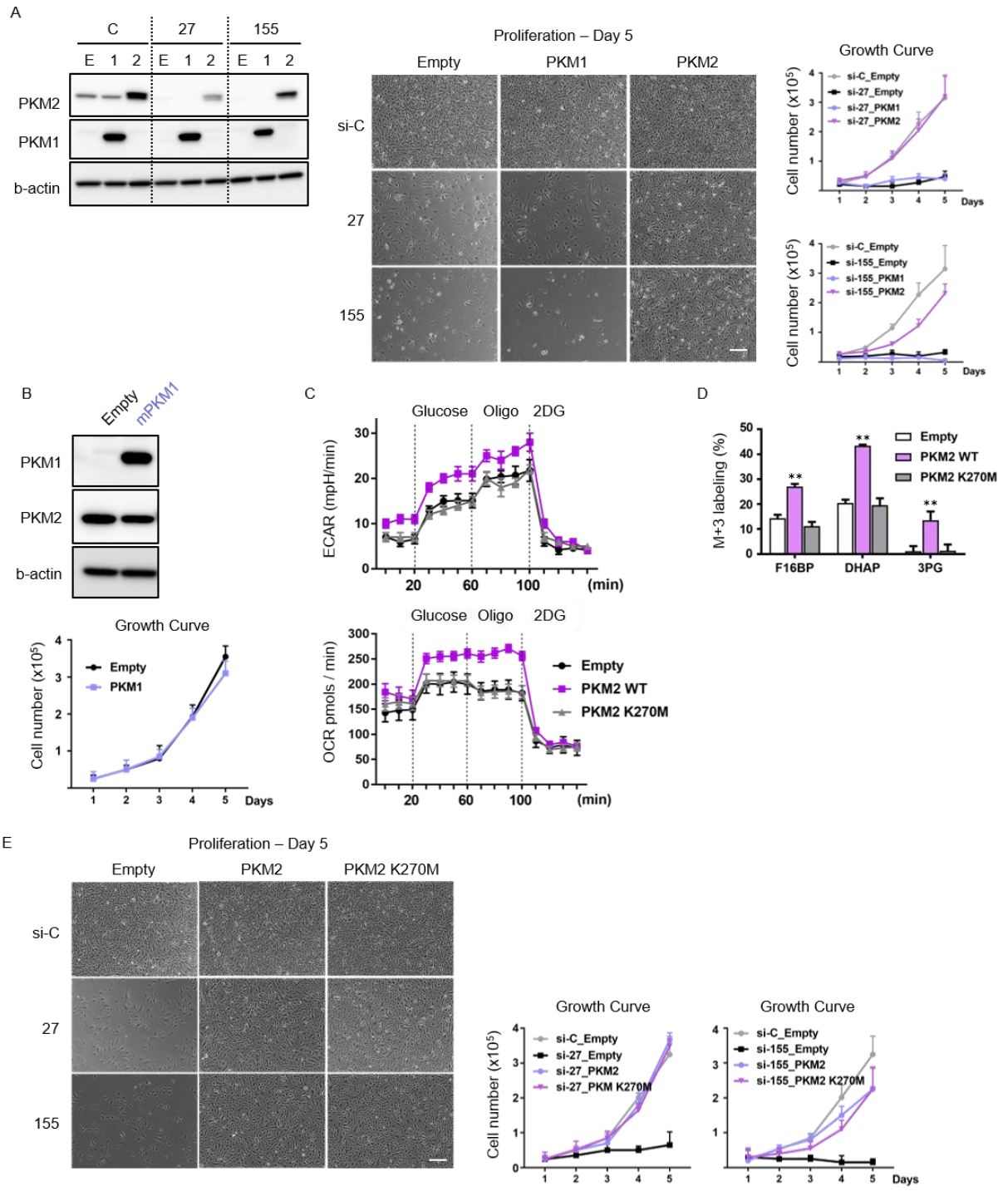

Supplementary Figure 4. Pyruvate kinase activity of PKM is dispensable for EC proliferation.

(A) Western blot analysis (left panel) and proliferation assay (middle and right panels) with overexpression of empty vector (E), PKM1 (1), or PKM2 (2) in the presence of si-27 or si-155. Cells were collected at the end of proliferation assay (day 5) and applied for western blot to

confirm stable overexpressions of PKM1 or PKM2. Scale bar = 100 μm. n = 4. (B) Western blot analysis (upper panel) and proliferation assay (lower panel) with overexpression of PKM1 without knockdown of endogenous PKM in HUVECs. n = 4. (C) ECAR and OCR during glycolysis test with glucose, oligomycin, and 2DG treatment. n = 8. (D) Glycolysis flux estimated by incorporation of [U-13C] glucose into M+3 labeling of fructose-1-6-bisphosphate (F16BP), dihydroacetone phosphate (DHAP), and 3-phosphoglycerate (3PG). n = 3. (E) Proliferation assay with overexpression of empty vector, PKM2 WT, or PKM2 PEP binding mutant (K270M) in the presence of si-27 or si-155. Scale bar = 100 μm. n = 4. All data are represented as mean ± STDEV. *P < 0.05. **P < 0.01, by two-tailed Student's t-test.

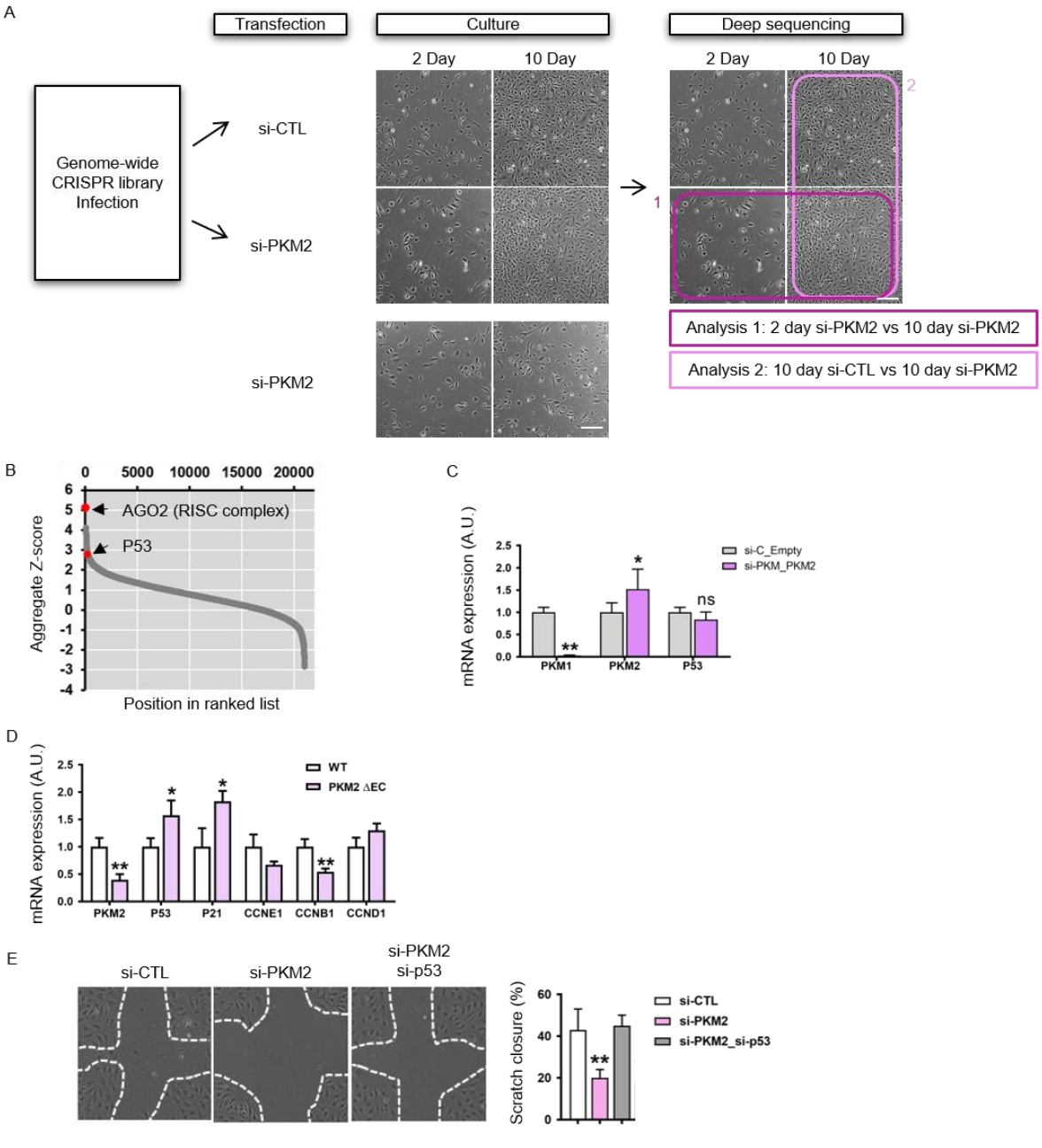

Supplementary Figure 5. Elevated p53 expression suppresses EC proliferation in PKM2 depleted ECs.

(A) Schematic of CRISPR screen. HUVECs were infected with genome-wide CRISPR library and transfected with either si-CTL or si-PKM2. Transfected cells were cultured for short (2 day) or long (10 day) period of time and then deep sequenced. Two different analysis were made: 1) 2 day after si-PKM2 vs 10 day after si-PKM2 (in purple) and 2) 10 day after si-CTL vs 10 day after si-PKM2 (in pink). Representative phase contrast cell pictures are shown after indicated time of cell culture in each condition. Scale bar = 100 µm. (B) The Z scores from the two different analysis above are combined and plotted as an Aggregate Z-score. Red dot on top

indicates AGO2, top #1 ranked, a major component of RISC complex. Red dot below indicates p53 that is ranked at top #179. (C) Reduced PKM1 expression does not alter p53 mRNA expression. p53 expression was compared in empty vector-overexpressing cells knocked down with si-C and PKM2-overexpressing cells knocked down with si-PKM, mimicking the effect of PKM1 knockdown. $n = 3$. (D) qPCR analysis in the ECs isolated from the lung of WT vs $PKM2^{\Delta EC}$ mice after tamoxifen injection. $n = 3$. (E) Knockdown of p53 rescues scratch closure in PKM2 knockdown ECs. $n = 4$. Scale bar = 100 μm. All data are represented as mean ± STDEV. $^{*}P < 0.05$. $^{**}P < 0.01$, by two-tailed Student's *t*-test.

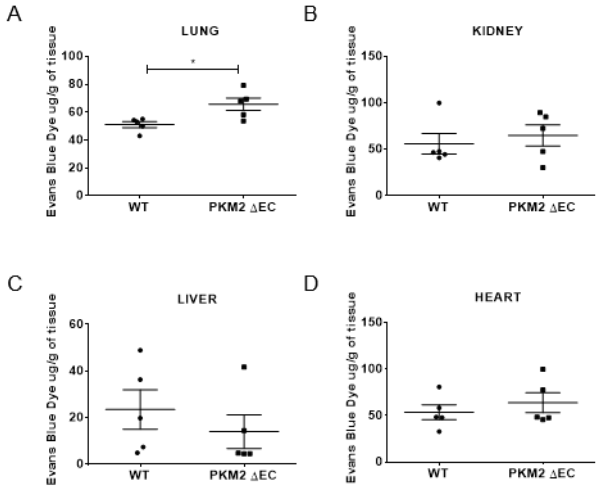

Supplementary Figure 6. PKM2$^{\Delta EC}$ mice demonstrate increased basal pulmonary microvascular permeability.

Basal vascular permeability was assessed in various organs 30 minutes after intravenous injection of Evans Blue dye. Quantification of extracted Evans Blue dye from lung (A), kidney (B), liver (C), and heart (D) in WT vs PKM2$^{\Delta EC}$ mice. Evans Blue dyes were normalized to tissue weight (µg of Evans Blue dye / g of tissue). Lung from PKM2$^{\Delta EC}$ mice shows significantly increased leakage compared to littermate control mice. n = 5 per group. All data are represented as mean ± STDEV. *P < 0.05, by two-tailed Student's t-test.

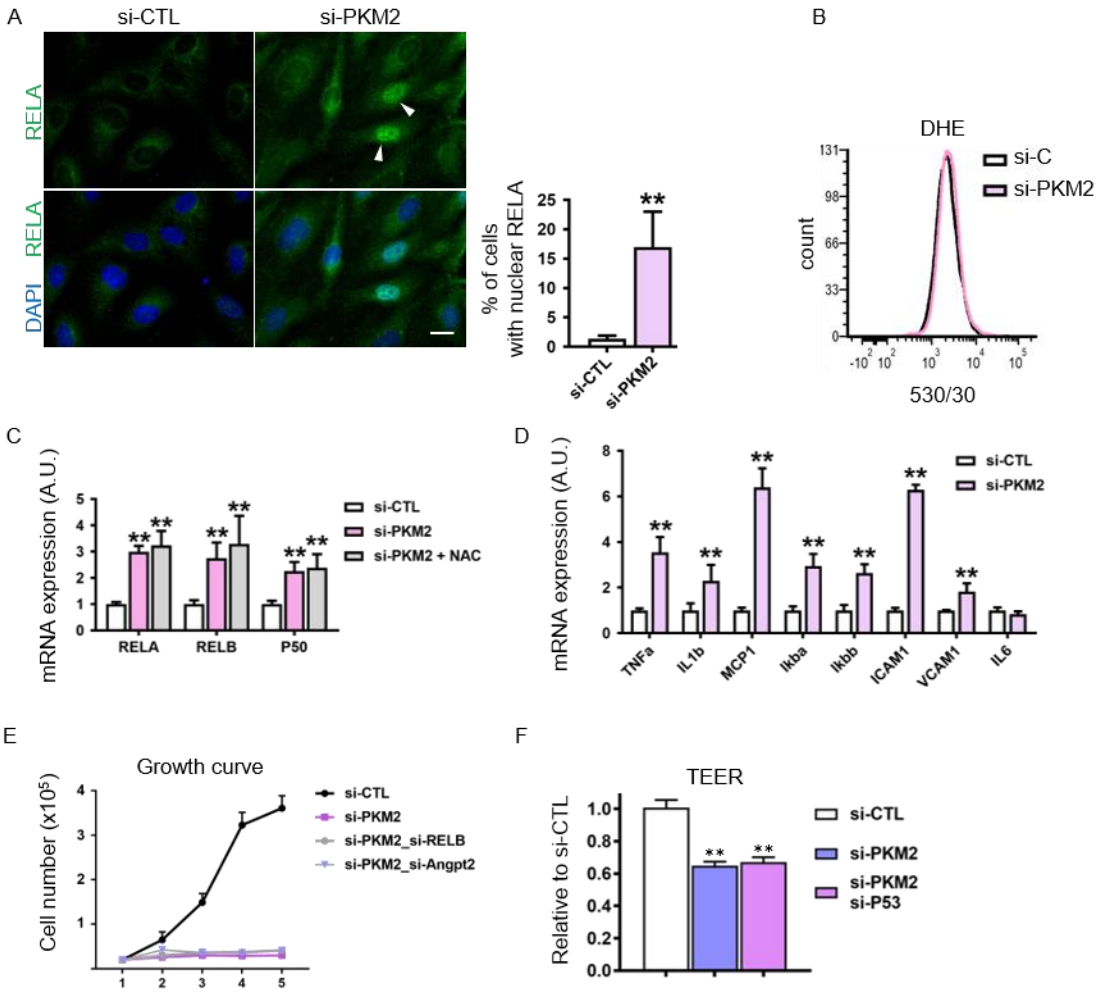

Supplementary Figure 7. PKM2 knockdown activates NF-kB independent of ROS production.

(A) Induction RELA localization into nucleus by PKM2 knockdown. Representative images showing co-staining of RELA (green) and DAPI (blue) (left panel) and quantification of the percentage of cells with nuclear RELB (right panel). n = 8. Scale bar = 10 μm. (B) ROS production was measured by DHE staining followed by flow cytometry in the ECs with si-CTL vs si-PKM2. The data represents 3 independent experiments. (C) qPCR analysis of NF-kB subunits in si-PKM2 ECs with or without NAC treatment. n = 3. (D) qPCR analysis of canonical downstream targets of NF-kB in the ECs with si-CTL vs si-PKM2. n = 3. (E) Proliferation assay with double knockdown of either RELB or Angpt2 on top of si-PKM2. n = 4. (F) TEER assay with double knockdown of p53 on top of si-PKM2. n = 4. All data are represented as mean ± STDEV. $^{**}P < 0.01$, by two-tailed Student's t-test.